Cement and Concrete Research 40 (2010) 526–530

Contents lists available at ScienceDirect

Cement and Concrete Research

journal homepage: http://ees.elsevier.com/CEMCON/default.asp

Influence of lithium hydroxide on alkali–silica reaction

D. Bulteel *, E. Garcia-Diaz, P. Dégrugilliers

Univ Lille Nord de France, F-59000 Lille, France
EMDouai, MPE-GCE, F-59500 Douai, France

ARTICLE INFO

Article history:
Received 3 November 2008
Accepted 19 August 2009

Keywords:
Alkali-silica reaction (C)
Reactive aggregate (D)
Reaction degree (A)
Lithium (D)
Inhibitor

ABSTRACT

Several papers show that the use of lithium limits the development of alkali–silica reaction (ASR) in concrete. The aim of this study is to improve the understanding of lithium's role on the alteration mechanism of ASR.

The approach used is a chemical method which allowed a quantitative measurement of the specific degree of reaction of ASR. The chemical concrete sub-system used, called model reactor, is composed of the main ASR reagents: reactive aggregate, portlandite and alkaline solution. Different reaction degrees are measured and compared for different alkaline solutions: NaOH, KOH and LiOH.

Alteration by ASR is observed with the same reaction degrees in the presence of NaOH and KOH, accompanied by the consumption of hydroxyl concentration. On the other hand with LiOH, ASR is very limited. Reaction degree values evolve little and the hydroxyl concentration remains about stable.

These observations demonstrate that lithium ions have an inhibitor role on ASR.

1. Introduction

It is well known that alkali–silica reaction (ASR) poses a durability problem to concrete. It can induce cracking and damage in concrete structures.

The origin of the reaction is a chemical reaction between three essential compounds included in concrete: moisture, a sufficiently high alkali concentration and a pessimum amount of reactive silica in the aggregate. The high alkali concentration will in turn produce a high hydroxyl ion concentration to maintain charge balance with the presence of portlandite. Different methods have been made to mitigate or prevent ASR. The addition of lithium salts is one of these methods. The first reported use of lithium salts to control ASR was in 1951 [1]. Since, many papers on mortar bars or concrete [2–10] have reported reducing or suppressive effects on expansion due to ASR. But the mechanism or mechanisms by which lithium acts, are not well understood [11]. Like Mitchell et al. [12], this work used a chemical concrete sub-system. In this study, the model reactors consisted of reactive aggregate, portlandite and alkaline solution: NaOH, KOH or LiOH. The aim of this study was to improve the understanding of lithium's role on the alteration mechanism of ASR by quantitative measurements of specific reaction degrees and alkaline species.

2. Materials and methods

2.1. Reactive aggregate used

The material used in this study was a “chert type” reactive aggregate from the north of France. This material was chosen due to its high reactivity so as to achieve a comparison of NaOH, KOH and LiOH action on ASR which is the aim of the study. Chemical and mineralogical characterisations were given by Bulteel et al. [13]. In summary X-ray fluorescence analysis gave a composition close to 99% SiO_2 (Table 1 with CO_2 value determined by thermogravimetric analysis). X-ray diffraction analysis detected only quartz lines in this aggregate. Elements other than Si were not studied. The quartz crystal lattice was characterised by ^{29}Si solid NMR spectroscopy [14]. This crystal lattice was constituted by Q_4 SiO_2 tetrahedra and Q_3 $SiO_{5/2}H$ “silanol” tetrahedra. The Q_3 molar fraction measured by thermogravimetry was close to 0.07.

The mineralogy of this aggregate was essentially micro to crypto crystalline (microquartz) and contained radial fibers (chalcedony). The crystal size was variable but in general particularly small: a few microns. However, a few grains presented a development of chalcedony zones. Carbonate fragments (calcite) were present in agreement with the low content in calcium measured by XRF (Table 1). In this way, the presence of iron oxide traces was also detected by XRF (Table 1).

The material had a specific area of 0.97 m^2/g by BET analysis and a specific porosity of 3 mm^3/g by BJH analysis. As the external surface calculated from size distribution data was as low as 0.008 m^2/g, the reactive sites of the studied aggregate were mainly located in a kind of

* Corresponding author. Univ Lille Nord de France, F-59000 Lille, France.
E-mail address: bulteel@ensm-douai.fr (D. Bulteel).

0008-8846/$ – see front matter © 2009 Elsevier Ltd. All rights reserved.
doi:10.1016/j.cemconres.2009.08.019

Table 1
Whole rock main element composition of the reactive aggregate in wt.% of oxides obtained by X-ray fluorescence analysis (XRF).

Main elements	wt.%
SiO_2	98.9
Fe_2O_3	0.4
CaO	0.3
CO_2 [a]	0.2
Al_2O_3	0.2
Sum	100.0

Species not listed are near or under LLD.
[a] CO_2 was measured gravimetrically as ignition loss LOI.

"internal surface". Its absolute density measured by helium pycnometer analysis was approximately 2.595 g/cm^3.

According to the literature [15,16], the potential reactivity of each silica type contained in this aggregate was classified high.

This aggregate was crushed to 0.16–0.63 mm and homogenized for this study.

2.2. Determination of reaction degrees

The determination of reaction degrees was based on the ASR mechanism which is described using different models [17–21] and can be written in two main steps (e.g. here for KOH):

Formation of Q_3 sites (step 1) due to attack of the first siloxane bonds by hydroxyl ions:

$$SiO_2 + KOH \rightarrow SiO_{5/2}K + 0.5H_2O. \tag{1}$$

From a structural point of view, SiO_2 represents a Q_4 silicon tetrahedron sharing 4 oxygens with 4 neighbours, and using a simplified wording, $SiO_{5/2}K$ represents the Q_3 tetrahedron sharing 3 oxygens with 3 neighbours.

Dissolution of silica (step 2) due to continued hydroxyl attack of the Q_3 sites to form Q_0 silica ions:

$$SiO_{5/2}K + KOH + 0.5H_2O \rightarrow (H_2SiO_4)^{2-} + 2K^+ \tag{2}$$

These silica ions respect the Iler equilibrium [22] according to pH.

Afterwards, precipitation of silica ions by the cations of the pore solution of concrete is likely to give C–S–H and/or C–K–S–H phase formation.

In this study, the use of the chemical method [14] allowed quantification of specific reaction degrees of ASR based on steps (1) and (2), which are defined as follows:

$$FMQ_4 = \text{moles of } Q_4 \text{ sites/moles of initial silica} \tag{3}$$

$$FMQ_3 = \text{moles of } Q_3 \text{ sites/moles of initial silica} \tag{4}$$

$$FMQ_0 = \text{moles of dissolved sites/moles of initial silica} \tag{5}$$

$$FMQ_4 + FMQ_3 + FMQ_0 = 1. \tag{6}$$

Formed Q_0 silica ions can remain in solution or can be precipitated:

$$FMQ_0 = FMQ_{0solution} + FMQ_{0precipitated} \tag{7}$$

$$FMQ_{0solution} = \text{moles of silica ions in solution/moles of initial silica} \tag{8}$$

$$FMQ_{0precipitated} = \text{moles of precipitated silica/moles of initial silica.} \tag{9}$$

2.3. Assessment of reaction degrees

2.3.1. General

The chemical method based on using a model reactor allowed the determination of reaction degrees, obtained by solid and liquid characterisations at different reaction times. The following protocol was used in the different procedures [23].

2.3.1.1. Start. A mixture of 1 g of 0.16–0.63 mm crushed aggregate and 0.5 g $Ca(OH)_2$ was introduced in a closed stainless steel container. After 30 minute preheating up to 80 °C, 10 ml of 0.79 mol/l KOH was added. The container was then autoclaved at different times at 80 °C to accelerate ASR under isothermal temperature.

2.3.1.2. Procedure 1. After the reaction, the aggregate is constituted by Q_4 tetrahedra that have not reacted (sound silica) and by the Q_3 tetrahedra (i.e. $SiO_{5/2}K$, $SiO_{5/2}CaSiO_{5/2}$ and $SiO_{5/2}H$) which constitute the degraded silica. In this procedure, approximately 50 to 75% of the alkaline solution was extracted and filtered to 0.45 µm. The solution's silica concentration ($FMQ_{0solution}$ defined in Eq. (8)) was determined by ICP-OES analyses after HNO_3 acidification with a Varian 720-ES instrument. Alkaline concentration was assessed by titration analyses. From these two parameters, hydroxyl concentration was determined [24].

Material from two different reaction vessels' was treated by two methods. The first was treated by Procedure 2a and the second by Procedure 2b.

2.3.1.3. Procedure 2a (acid alternative). Selective acid digestion with 250 ml cold 0.5 M HCl solution followed by filtration leads to the removal of the soluble reaction products ($(H_2SiO_4)^{2-}$, $(H_3SiO_4)^-$, K^+, Ca^{2+}, C–S–H and/or C–K–S–H) but also reagents (KOH and $Ca(OH)_2$). During this chemical treatment the Q_3 tetrahedra $SiO_{5/2}K$ and/or $SiO_{5/2}CaSiO_{5/2}$ are protonated to form silanols $SiO_{5/2}H$ with a release of K^+ and/or Ca^{2+} cations.

The acid rinse was considered as successful when the remaining solid contained more than 99% of SiO_2 measured by X-ray fluorescence. In this case, measurements of the remaining solid characterised by ^{29}Si solid NMR spectroscopy showed residual SiO_2 Q_4 tetrahedra and $SiO_{5/2}H$ Q_3 tetrahedra and confirmed the absence of silica gel precipitation after the acid treatment [14].

After thermal treatment of the residual solid at 1000 °C, the silanol groups were condensed to give back silica Q_4 and release water following:

$$2SiO_{5/2}H \xrightarrow{1000\,^\circ C} 2SiO_2 + H_2O. \tag{10}$$

Measurement of the water loss by thermogravimetry allowed calculation of the quantity of Q_3 tetrahedra in the aggregate sample (FMQ_3 defined in Eq. (4)). The weight of the residual silica made it possible to determine by difference the quantity of dissolved silica (FMQ_0 defined in Eq. (5)). With silica concentration in the solution measured according to Procedure 1 ($FMQ_{0solution}$), precipitated silica ($FMQ_{0precipitated}$) was determined by Eq. (7).

2.3.1.4. Procedure 2b (alkaline alternative). Filtration with ethyl alcohol allowed to preserve solid and mainly $Ca(OH)_2$. Measurement of the mass loss by thermogravimetry (about 450 °C for the dehydration of portlandite specifically and sometimes about 700 °C for the CO_2 loss in the case of carbonated portlandite for the experiment) allowed the calculation of the quantity of residual portlandite and so the content of consumed portlandite.

The experimental procedure above for KOH was duplicated using either NaOH or LiOH solution. Results from all three runs are given below.

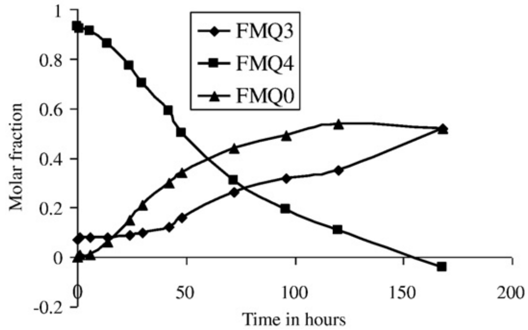

Fig. 1. Molar fractions of Q_4, Q_3 and Q_0 according to time for the model reactor with KOH.

3. Results

3.1. Reaction progress with time

The variation of molar fractions FMQ_4, FMQ_3 and FMQ_0 with time as shown in Figs. 1, 2 and 3 demonstrates the very different effects of LiOH compared to NaOH and KOH. Globally, the molar fraction evolution is similar for KOH and NaOH. Q_4 tetrahedra are highly consumed by hydroxyl attack. Moreover in the case of KOH, the assumption based on a representation of the aggregate only with Q_3 and Q_4 tetrahedra gives a limit with the "negative value" for FMQ_4 in Fig. 1. Indeed, at a very high alteration, the presence of Q_2 sites is no longer negligible, hence a bad value of FMQ_4. FMQ_0 increased up to 72 and 120 h respectively for NaOH and KOH to reach an asymptotic value of about 0.5. The content of Q_3 sites increased after a short plateau of about 24 h which corresponds to the initial Q_3 sites value ($FMQ_3 \approx 0.07$). On the other hand, the molar fractions evolution from LiOH was totally different. FMQ_4 passed from 0.93 to about 0.8 indicating only a small consumption by hydroxyl attack. In addition, Q_3 and Q_0 quantities formed were very small with FMQ_3 from 0.07 to about 0.15 and FMQ_0 close to 0.06 in spite of a longer time of attack (336 h).

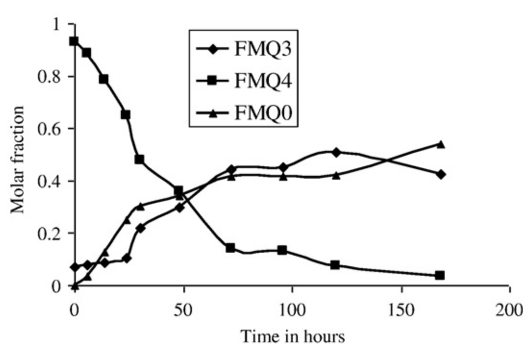

Fig. 2. Molar fractions of Q_4, Q_3 and Q_0 according to time for the model reactor with NaOH.

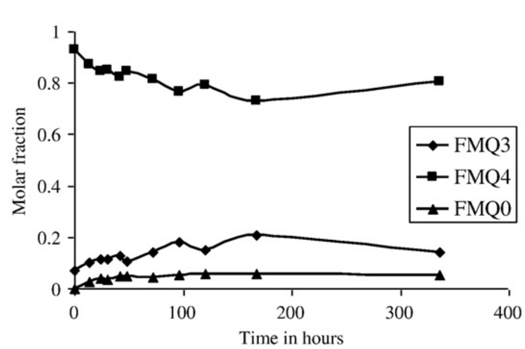

Fig. 3. Molar fractions of Q_4, Q_3 and Q_0 according to time for the model reactor with LiOH.

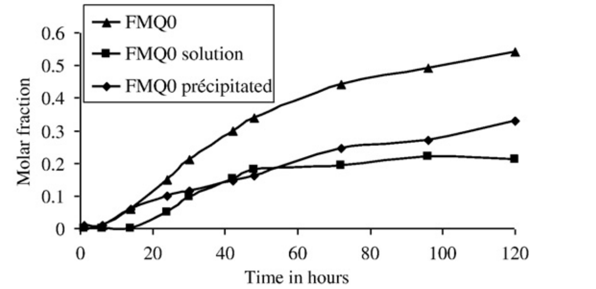

Fig. 4. Molar fraction of Q_0 constituted to molar fractions of $Q_{0solution}$ and $Q_{0precipitated}$ according to time for the model reactor with KOH.

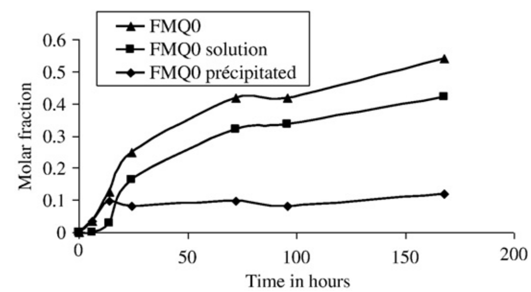

Fig. 5. Molar fraction of Q_0 constituted to molar fractions of $Q_{0solution}$ and $Q_{0precipitated}$ according to time for the model reactor with NaOH.

Figs. 4, 5 and 6 show FMQ_0 dissolved silica evolution which corresponds to $FMQ_{0solution}$ free silica ions in solution and $FMQ_{0precipitated}$ precipitated silica (Eq. (7)) according to time. With KOH and NaOH, FMQ_0 increased up to 0.5. Between 0 and 14 h, dissolved silica precipitated but after 14 h, free silica ions appeared and increased while the precipitation continued in the case of KOH and remained stable in the case of NaOH. With LiOH, the result was completely different. FMQ_0 was not higher than 0.06 and all dissolved silica ions precipitated.

Q_3 sites content according to dissolved silica is shown in Fig. 7. For KOH and NaOH, the curves are generally similar. In the first part, dissolved silica formation was favoured with FMQ_0 increasing from 0 to close to 0.3 while FMQ_3 had increased from 0.07 to 0.1 only. In the second part, Q_3 site content was increased by 5 to 7 in comparison with the initial value. Inversely, with LiOH, the cloud of points close to the origin shows a very small content of FMQ_0 and FMQ_3 that only increased by a factor of 2.

3.2. Evolutions of alkaline species

Figs. 8, 9 and 10 show evolutions of 3 alkaline species: alkaline concentration, hydroxyl concentration and consumption of portlandite

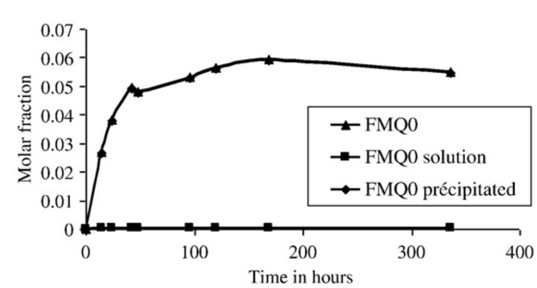

Fig. 6. Molar fraction of Q_0 constituted to molar fractions of $Q_{0solution}$ and $Q_{0precipitated}$ according to time for the model reactor with LiOH.

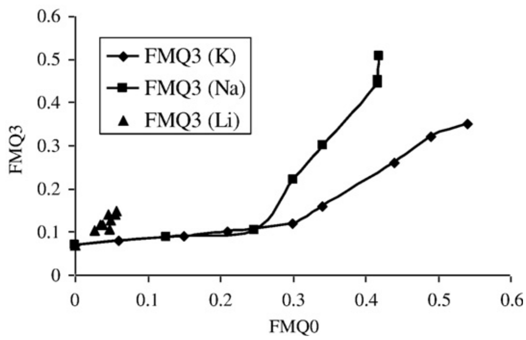

Fig. 7. Molar fraction of Q_3 sites according to molar fraction of dissolved silica for 3 model reactors: KOH, NaOH and LiOH.

according to the molar fraction of dissolved silica (FMQ_0). At different reaction degrees, alkaline species evolution was visible enough with KOH and NaOH compared to LiOH. In Fig. 8 (KOH), after a short plateau, $FMQ_0=0.06$, hydroxyl concentration fell throughout the reaction. Up to $FMQ_0=0.2$, the alkaline concentration was relatively stable then decreased from 0.76 to 0.54. Consumption of portlandite increased for the reaction to reach more than 0.8. In Fig. 9 (NaOH), the alkaline concentration evolved between 0.79 and 0.7. Hydroxyl concentration fell very quickly to reach about 10^{-4} mol/l. Consumption of portlandite continuously increased to reach close to 0.9. In the case of LiOH (Fig. 10), the evolution of alkaline species was totally different as it makes almost no progress; FMQ_0 did not exceed 0.06 instead of 0.6 for the two other

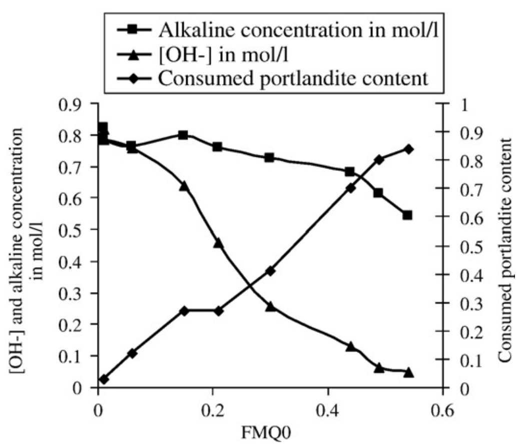

Fig. 8. Hydroxyl concentration, alkaline concentration and consumption of portlandite according to molar fraction of dissolved silica for KOH model reactor.

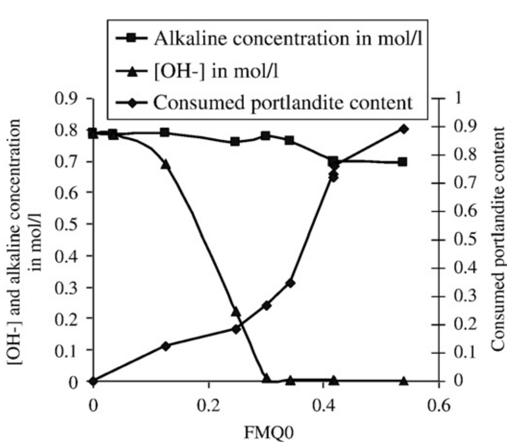

Fig. 9. Hydroxyl concentration, alkaline concentration and consumption of portlandite according to molar fraction of dissolved silica for NaOH model reactor.

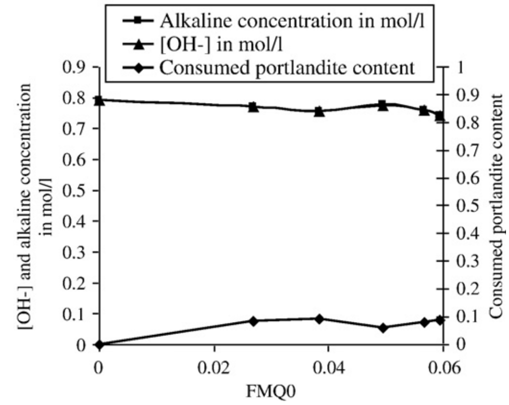

Fig. 10. Hydroxyl concentration, alkaline concentration and consumption of portlandite according to molar fraction of dissolved silica for LiOH model reactor.

cases. Alkaline concentration and hydroxyl concentration were identical and remain at high values: 0.75 mol/l. Portlandite content was little consumed (less than 0.1).

4. Discussion

The aim of this study was to improve the understanding of lithium's role on the alteration mechanism of ASR by comparative study between different alkaline species (Na, K and Li) on quantitative measurements of specific reaction degrees. To do this comparison, model reactors were used with one reactive aggregate and the same hydroxyl concentration without mixing alkaline species. In this case of the model reactor, the hydroxyl concentration was controlled and resulted in the use of LiOH. But in concrete, usual additions are lithium salts like $LiNO_3$ [25] to avoid the increase in hydroxyl ions provided with LiOH. The study of other lithium salts will be the subject of future investigations.

Through all the results of this study, two different behaviours were observed. On the one hand, model reactors with KOH and NaOH presented a similar evolution and will be discussed together and on the other hand, the model reactor with LiOH was very different and will be compared to the two others.

In the cases of KOH and NaOH (Figs. 1 and 2), Q_4 molar fraction fell while Q_3 and Q_0 molar fractions increased and as a result ASR progressed. Indeed, from Eqs. (1 and 2), the Q_4 sites give Q_3 sites and Q_0 dissolved silica. This high proportion of final dissolved silica shows that Eq. (2) plays an important part in this experiment where the initial hydroxyl concentration is high at 0.79 mol/l. The high content of Q_3 sites was characteristic of a silica gel formed by the hydroxylic break-up of the siloxane bonds, probably following a topochemical mechanism. The large increase of FMQ_3 showed that the creation of Q_3 sites prevailed over the dissolution reaction in spite of high FMQ_0 (Fig. 7). Eq. (1) is greater than Eq. (2). From Eqs. (1 and 2), the development of ASR also consumes hydroxyl ions (Figs. 8 and 9) involving a reduction in hydroxyl concentration and portlandite consumption. Indeed, the reduction in hydroxyl concentration involves an increase of portlandite solubility which supplies hydroxyl ions available for the reaction and also releases calcium ions. Then, these calcium ions take part in the precipitation of dissolved silica in the form of C–S–H which also could trap alkalis (Figs. 4 and 5). In these cases, the reaction is so developed that all dissolved silica do not precipitate and remain in solution. The alkaline concentration remained relatively high because the consumption of (OH^-) hydroxyl ions was balanced by the appearance of silica ions in solution ($(H_2SiO_4)^{2-}$ and/or $(H_3SiO_4)^-$).

In the case of LiOH, reaction degrees (specific to ASR) and alkaline species were completely different. They evolved slightly compared to KOH and NaOH. Indeed, FMQ_4, FMQ_3 and FMQ_0 change only a slightly

(Fig. 3) indicating a very small hydroxyl attack according to Eqs. (1 and 2) despite a high concentration with 0.79 mol/l. Thus, few Q_3 sites and Q_0 dissolved silica were formed (Fig. 7). The hydroxyl concentration remained high due to a lack of the hydroxylic break-up of the siloxane bonds (Fig. 10). Portlandite which played the role of hydroxyl reserve was scarcely consumed. A very small quantity of dissolved silica was totally and immediately precipitated with calcium ions (Fig. 6). The absence of silica concentration in solution gave an alkaline concentration equal to the hydroxyl concentration. These results agree with the reduction or suppression of silica dissolution observed by Tremblay et al. [26] with the use of lithium salt (like $LiNO_3$) on reactive silica in other experiments.

These results show that ASR progresses very little in the presence of LiOH even for a very long time in very severe conditions in the model reactor. In these conditions, LiOH was an inhibitor of ASR.

In previous research [27], the authors of this manuscript proposed an ASR mechanism where expansion was related to an increase of FMQ_3. In this study, LiOH induced relatively fewer Q_3 sites and resulted in a low expansion risk. But the problem is how can the very small quantity of formed products with such a high hydroxyl concentration with 0.79 mol/l be explained whereas with NaOH and KOH, it was quite sufficient to develop ASR? After Feng et al. [11,28] in which a different mechanism was assumed, a small quantity of formed products would have no expansive nature and would perhaps form a “barrier” to stop hydroxyl attack. On this assumption, a low initial reaction would produce few products including lithium. These products would prevent hydroxyl attack and thus Q_3 sites formation and result in a low expansion risk.

5. Conclusions

The use of model reactors constituted from reactive aggregate, portlandite and alkaline solution like NaOH, KOH or LiOH and cured at 80 °C allowed the most favourable conditions to develop ASR and to directly compare between the effects of different alkaline species. This study measured specific and quantitative ASR reaction degrees and also alkaline species. The results led to the following conclusions:

(1) With NaOH and KOH, reaction degrees and alkaline species evolved greatly and hence ASR developed. On the other hand, with LiOH, the result was totally different as the reaction degrees and alkaline species showed small evolutions. ASR progressed very little and showed LiOH as an inhibitor of ASR.

(2) In literature, the absence of expansion on mortar bars or concretes with LiOH could be explained by the reduction/suppression of silica dissolution [23] but above all due to low formation of Q_3 sites in the aggregate. Indeed, in previous work [27], the authors proposed the ASR mechanism where expansion was in relation with the increase of Q_3 sites. LiOH induces relatively fewer Q_3 sites and results in a low expansion risk.

(3) LiOH inhibits ASR because the quantity of formed ASR products was very small. However it is still unclear why are there so few ASR products in combination with such a high hydroxyl concentration (0.79 mol/l)? In the case of NaOH and KOH, these same conditions were quite sufficient to develop ASR. It is possible that a small quantity of formed products would have no expansive nature and would perhaps form a “barrier” to stop hydroxyl attack [28]. Future investigations will try to develop the identification of formed products for a better comprehension of the mechanism(s).

In this first study, LiOH was used because the model reactor allowed to control the hydroxyl concentration. Future investigations will also use lithium salts such as $LiNO_3$ which are more commonly used in concrete.

References

[1] W.J. McCoy, A.G. Caldwell, New approach to inhibiting alkali aggregate expansion, J. Am. Concr. Inst. 22 (1951) 693–706.
[2] D.C. Stark, Lithium salt admixtures — an alternative method to prevent expansive alkali–silica reactivity, Proceedings of the 9th ICAAR, 1992, pp. 1017–1025, London, UK.
[3] J.S. Lumley, ASR suppression by lithium compounds, Cem. Concr. Res. 27 (1997) 235–244.
[4] V.S. Ramachandran, Alkali-aggregate expansion inhibiting admixtures, Cem. Concr. Comp. 20 (1998) 149–161.
[5] S. Diamond, S. Ong, The mechanisms of lithium effects on ASR, Proceedings of the 9th ICAAR, 1992, pp. 269–278, London, UK.
[6] M.D.A. Thomas, R. Hooper, D. Stokes, Use of lithium-containing compounds to control expansion in concrete due to alkali–silica reaction, Proceedings of the 11th ICAAR, 2000, pp. 783–792, Quebec, Canada.
[7] M. Kawamura, T. Kodera, Effects of externally supplied lithium on the suppression of ASR expansion in mortars, Cem. Concr. Res. 35 (2005) 494–498.
[8] X. Mo, Laboratory study of LiOH in inhibiting alkali–silica reaction at 20 °C: a contribution, Cem. Concr. Res. 35 (2005) 499–504.
[9] X. Mo, T. Jin, G. Li, K. Wang, Z. Xu, M. Tang, Alkali-aggregate reaction suppressed by chemical admixture at 80 °C, Constr. Build. Mater. 19 (2005) 473–479.
[10] C.L. Collins, J.H. Ideker, G.S. Willis, K.E. Kurtis, Examination of the effects of LiOH, LiCl, and $LiNO_3$ on alkali–silica reaction, Cem. Concr. Res. 34 (2004) 1403–1415.
[11] X. Feng, M.D.A. Thomas, T.W. Bremner, B.J. Balcom, K.J. Folliard, Studies on lithium salts to mitigate ASR-induced expansion in new concrete: a critical review, Cem. Concr. Res. 35 (2005) 1789–1796.
[12] L.D. Mitchell, J.J. Beaudoin, P. Grattan-Bellew, The effects of lithium hydroxide solution on alkali silica reaction gels created with opal, Cem. Concr. Res. 34 (2004) 641–649.
[13] D. Bulteel, N. Rafai, P. Degrugilliers, E. Garcia-Diaz, Petrography study on altered aggregate by alkali–silica reaction, Mater. Charact. 53 (2004) 141–154.
[14] D. Bulteel, E. Garcia-Diaz, C. Vernet, H. Zanni, Alkali–silica reaction: a method to quantify the reaction degree, Cem. Concr. Res. 32 (2002) 1199–1206.
[15] M.A.T.M. Broekmans, Structural properties of quartz and their potential role for ASR, Mater. Charact. 53 (2004) 129–140.
[16] J.M. Ponce, O.R. Batic, Different manifestations of the alkali–silica reaction in concrete according to the reaction kinetics of the reactive aggregate, Cem. Concr. Res. 36 (2006) 1148–1156.
[17] L.S. Dent Glasser, N. Kataoka, The chemistry of alkali-aggregate reaction, Cem. Concr. Res. 11 (1981) 1–9.
[18] A.B. Poole, Alkali silica reactivity mechanisms of gel formation and expansion, Concrete Society Publications CS, Proceedings of the 9th ICAAR, 1992, pp. 782–789, London, UK.
[19] S. Urban, Alkali silica and pozzolanic reactions in concrete, Part 1: Interpretation of published results and a hypothesis concerning the mechanism, Cem. Concr. Res. 17 (1987) 141–152.
[20] H. Wang, J.E. Gillott, Mechanism of alkali–silica reaction and significance of calcium hydroxide, Cem. Concr. Res. 21 (1991) 647–654.
[21] R. Dron, Thermodynamique de la reaction alkali–silice, Bulletin de liaison des Laboratoires des Ponts et Chaussées 166 (1990) 55–59.
[22] R.K. Iler, The Chemistry of Silica, Wiley-Interscience Publication, New York, USA, 1979, 835 pp.
[23] D. Bulteel, J. Riche, E. Garcia-Diaz, N. Rafai, N.P. Degrugillers, Better understanding of ASR mechanism thanks to petrography study on altered flint aggregate, Proceedings of the 12th ICAAR, 2004, pp. 69–78, Beijing, China.
[24] D. Bulteel, Quantification de la réaction alkali–silice: application à un silex du Nord de la France, PhD thesis, Université des sciences et technologies de Lille, France, 2000, 301 pp.
[25] A. Santos Silva, M. Salta, M.E. Melo Jorge, M.P. Rodrigues, A.F. Cristino, Research on the suppression expansion due to ASR. Effect of coatings and lithium nitrate, Proceedings of the 13th ICAAR, 2008, pp. 1250–1260, Trondheim, Norway.
[26] C. Tremblay, M.A. Bérubé, B. Fournier, M.D.A. Thomas, K.J. Folliard, Experimental investigation of the mechanisms by which $LiNO_3$ is effectiveness against ASR, Proceedings of the 13th ICAAR, 2008, pp. 512–521, Trondheim, Norway.
[27] E. Garcia-Diaz, J. Riche, D. Bulteel, C. Vernet, Mechanism of damage for the alkali–silica reaction, Cem. Concr. Res. 36 (2006) 395–400.
[28] X. Feng, M.D.A. Thomas, B.J. Bremner, K.J. Folliard, B. Fournier, Summary of research on the effect of LiNO3 on alkali–silica reaction in new concrete, Cem. Concr. Res. 40 (2010) 636–642 (this issue).